Bilayer Formation between Lipid-Encased Hydrogels Contained in Solid Substrates

Stephen A. Sarles,[†] L. Justin Stiltner,[‡] Christopher B. Williams,[‡] and Donald J. Leo*,[†]

Center for Intelligent Material Systems and Structures (CIMSS), Department of Mechanical Engineering, and Design, Research, and Education for Additive Manufacturing Systems (DREAMS) Laboratory, Department of Mechanical Engineering, Department of Engineering Education, Virginia Tech, Blacksburg, Virginia 24061, United States

ABSTRACT Solidified biomolecular networks that incorporate liquid-supported lipid bilayers are constructed by attaching lipid-encased, water-swollen hydrogels contained in oil. Poly(ethylene glycol) dimethacrylate (PEG-DMA) and a free-radical photoinitiator are added to an aqueous lipid vesicle solution such that exposure to ultraviolet light results in solidification of neighboring aqueous volumes. Bilayer formation can occur both prior to photopolymerization with the aqueous mixture in the liquid state and after solidification by using the regulated attachment method (RAM) to attach the aqueous volumes contained within a flexible substrate. In addition, photopolymerization of the hydrogels can be performed in a separate mold prior to placement in the supporting substrate. Membranes formed across a wide range of hydrogel concentrations [0−80 % (w/v); MW = 1000 g/mol PEG-DMA] exhibit high electrical resistances (1−10 GΩ), which enable single-channel recordings of alamethicin channels and show signficant durability and longevity. We demonstrate that just as liquid phases can be detached and reattached using RAM, reconfiguration of solid aqueous phases is also possible. The results presented herein demonstrate a step toward constructing nearly solid-state biomolecular materials that retain fluid interfaces for driving molecular assembly. This work also introduces the use of three-dimensional printing to rapidly prototype a molding template used to fabricate polyurethane substrates and to shape individual hydrogels.

KEYWORDS: lipid bilayer • hydrogel • poly(ethylene glycol) • solidified biomolecular assemblies • regulated attachment method • alamethicin

INTRODUCTION

The formation of bioinspired assemblies, such as proteoliposomes and supported lipid bilayers, provides scientists and engineers with a means of constructing artificial membranes that mimic the structure and properties of living cell membranes. These platforms have historically provided a suitable in-laboratory approach for studying the properties of lipid bilayers, examining the functionality of specific transmembrane proteins, and even performing analyte sensing (1−3) for drug screening and DNA base-pair analysis (4−6) using modified ion channels.

An alternative perspective of these material systems is one that strives not to achieve a single lipid bilayer interface for studies that are designed to last a few hours but instead to create durable cell-inspired material systems that feature networks of functional membranes. Key challenges in this progression toward building cell-network-inspired material systems are the development of ways to *assemble*, *package*, and *stabilize* the various components of the system. These same principles are instrumental to the growth and survival of living cells: molecules are first synthesized and assembled, they are then packaged into units (vacuoles, organelles, vesicles), and finally they are transported to regions in the cells where their functions and structures act to stabilize the

viability of the cell. Recent work in our group has specifically focused on addressing these issues in order to develop novel engineering platforms that retain the inherent functionality of biological molecules.

First, our group introduced a new method for assembling encapsulated interface bilayers in situ within flexible, solid substrates (7). This method of bilayer formation was termed the regulated attachment method (RAM) because contact between adjacent lipid-encased aqueous volumes surrounded by oil and contained within a solid substrate is regulated by changing the internal dimensions of the substrate. The application of force on the substrate creates a controlled deformation that enables volumes to be connected and reconnected to form lipid bilayers. One difference between this technique and the droplet interface bilayer (DIB), where bilayers form at the interfaces of lipid-encased aqueous droplets (8, 9), is the ability to control the size of the interface bilayer independently of the size of the aqueous volumes by controlling the dimensions of the compartments with the applied force. A second benefit of RAM is the ability to change the composition of the aqueous volumes, and thus the bilayer, by incorporating new species delivered in aqueous packets injected through the oil phase - a process that we showed can be performed even after bilayer formation (7).

In a parallel article, we demonstrated that the physical encapsulation of interface bilayers within solid substrates produces durable and more-portable packaged biomolecular assemblies compared to traditional DIBs. This work demonstrated that with *encapsulation* a thin layer of oil separating

the aqueous volumes from the rigid acrylic substrate provides additional support to the assembly while still retaining a fluid oil/water interface necessary for sufficient lipid monolayer assembly (10). Additional features such as integrated electrodes and a solid cap creates a packaged biomolecular material system capable of being handled, shaken, and even fully inverted.

While previous works with liquid-supported interface bilayers have used either aqueous droplets (8, 9, 11–14) or confined aqueous volumes (7, 15), building material platforms from liquid volumes requires either dispensing and manipulating discrete droplets or constructing substrates with internal compartments that produce the appropriate phase separation in situ. Our own experience in working with encapsulated interface bilayers demonstrated that, for spherical-shaped or near-spherical-shaped compartments, aqueous volumes can be shaped and distorted by the deformable substrate fairly easily (7). This characteristic is key to the success of the RAM for separating and then reattaching aqueous volumes held within a substrate. However, when the internal compartments are nonspherical, additional challenges arise in maintaining a desired geometry of the aqueous volumes (15). The breakup of an elongated volume into multiple smaller spheres, though widely used to create discrete droplets in microfluidic applications (16–19), interrupts the conductive pathway by creating unwanted interface bilayers or disconnected aqueous volumes separated by oil in liquid biomolecular networks.

The anticipated advantages of assembling solid-phase aqueous volumes include the ability to physically confine the liquid aqueous phase within the overall shape of the cross-linked gel instead of the substrate compartment geometry. As with liquid biomolecular assemblies, the boundary of each gel structure still provides the oil/water interface necessary for stabilizing the lipid monolayers that form the two leaflets of the interface bilayer. Thus, a hydrogel aqueous phase provides a convenient alternative to a liquid phase, where the overall shape is dictated by the dimensions of the gel and the mechanical properties of the gel can be tailored with composition and concentration in the aqueous medium (16, 20, 21). While the difference between a liquid aqueous phase and a water-swollen gel is subtle, the advantages of incorporating hydrogel materials into the aqueous phase provide many benefits that a pure liquid solution may not offer. Hydrogels, such as poly(ethylene glycol) (PEG) polymers, provide a bioinert medium for hosting a wide range of biological molecules (20, 22, 23) and have thus found use as synthetic cellular scaffolds (24, 25), drug-delivery materials (20, 26, 27), and biosensors (23, 28). Within biomolecular assemblies, the structure of the gel can be used to immobilize enzymes, host growth factors for scaffolding, provide binding sites for cells and proteins, and facilitate the controlled release of chemical species (29) to interact with specific interface bilayers. The gel itself can also respond to environmental changes such as pH or temperature, which can provide additional routes for sensing and mechanical actuation within each "block" (20, 29). Finally, the macro-scopic solidity of a water-swollen gel provides mechanical strength to the material assembly while retaining the necessary fluidity at much smaller length scales. Furthermore, the use of gels enables the fabrication of nonspherical shapes, expanding the possibilities of how networks can be arranged and contained within a durable material. In this way, the shape of the gel is maintained in both air and water and provides a three-dimensional (3D) wick for containing aqueous solutions.

The water-swollen nature of hydrogel scaffolds has also been used to encase suspended bilayers formed across the pore of a solid substrate (30–32), support bilayers formed between hydrogels at the end of a pipet (33), and comprise the lower aqueous support layer for a droplet on hydrogel bilayers developed by Wallace's group (34–36). These previous studies provide evidence not only that the presence of the hydrogel serves to stabilize the bilayer, making it more storable and resilient to failure (31, 32), but also that a key property of the lipid bilayer, membrane fluidity, is maintained even in close proximity to the more-solid gel structure.

In this paper, we demonstrate the concept of attaching lipid-encased hydrogels as an alternative approach for creating functional and modular biomolecular material systems stabilized within durable materials. The assembly of these systems specifically strives to create methods for developing cell-network-inspired materials, where lipid-encased hydrogels connected by interface bilayers mimic the connectivity of living cells and demonstrate the advantages of modularity and collective utility found in networks of liquid-supported interface bilayers. The results presented herein describe the formation and characterization of encapsulated interface bilayers formed via RAM between photopolymerizable PEG hydrogels. Specifically, aqueous volumes containing photopolymerizable PEG monomer, photoinitiator, and phospholipid vesicles become encased in a lipid monolayer when submerged in immiscible oil. Upon exposure to ultraviolet (UV) light, the water-soluble polymer cross-links to form a water-swollen hydrogel, where the material properties of the gel (i.e., viscosity, modulus) are dependent on the composition and curing regime of the polymer network. The RAM is used to attach, detach, and reattach the lipid-encased gels contained within the polyurethane (PU) substrates.

METHODS AND MATERIALS

3D Printing Technologies for Substrate Fabrication. 3D printing is used to produce PU substrates that are designed to encapsulate the solidified biomolecular networks studied in this work. The printed templates are designed to function much like ice-cube trays, where the negative spaces in the printed mold define the resulting hydrogel compartment geometries of the substrates used to hold the biomolecular assemblies (Figure 1a). An Objet Connex 350, which employs a direct 3D printing technique, is used to create the templates. The 3D printer builds 3D parts from a computer-aided design (CAD) file in a layer-by-layer fashion through the inkjet deposition of photopolymerizable materials that are solidified via immediate UV irradiation. The Connex 350 printer is chosen for this work primarily for its high resolution and surface finish. Printed polymer droplets are 42 μm in diameter (600dpi X–Y resolution), thus enabling the construction of templates with features ranging from 100

(a)

(b)

(c)
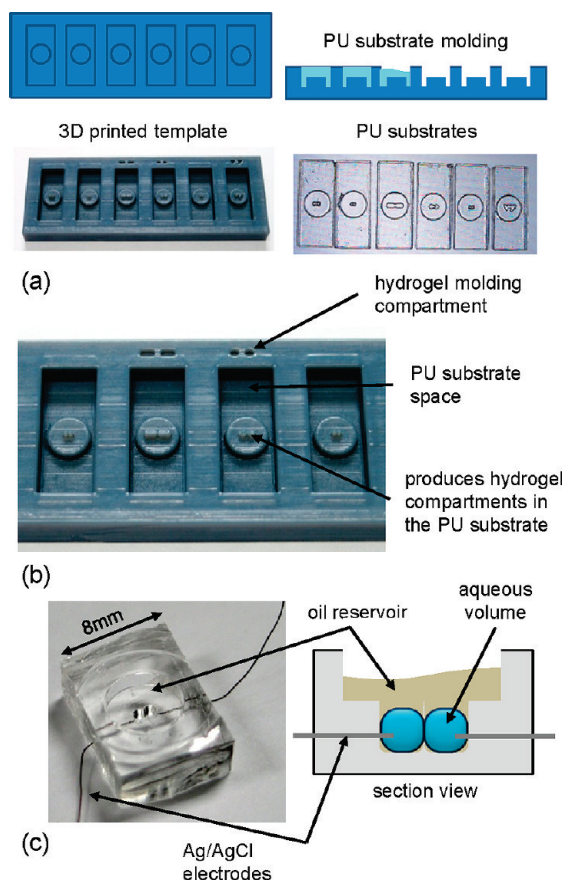
FIGURE 1. (a) Substrate templates rapidly prototyped using 3D printing technology used to form PU substrates through a single-molding step. (b) Features designed into the negative space of the template used to define the hydrogel compartments of the resulting PU substrates. Small wells in the template are also incorporated for shaping hydrogels prior to placing them into the substrates. (c) Finished PU substrates featuring recessed compartments (1 mm circular compartments are shown) for holding the aqueous phases, an upper reservoir for containing excess oil, and silver—silver chloride electrodes positioned within the compartments for electrical measurements.

to 1000 μm. The printer also provides the smallest layer thickness of all commercial rapid prototyping machines (16 μm); this produces a smooth finish on vertical surfaces, which ensures easy removal of the molded substrates.

In addition, the Connex 350 printer is the only commercially available printer that is able to simultaneously print multiple materials, thus providing a designer with the ability to tailor the stiffness and surface properties of the printed part. For this work, the template is printed using VeroGray60 (Digital Material 8530; elastic modulus $E = 1750$ MPa), a predefined ratio of Objet's TangoBlackPlus (FullCure 980; $E = 0.15-0.26$ MPa; shore hardness 27A), a flexible, rubberlike material, and VeroWhite (FullCure 830; $E = 2495$ MPa; shore hardness 83D), a white rigid plastic. The finished template shown in Figure 1a,b exhibits slight flexibility and a smooth surface finish necessary for accurate PU substrate casting.

The 3D printing approach allows the design of a substrate and subsequent template printing and substrate molding to occur within only a few hours from start to finish. This method eliminates the need to first machine the substrate features into acrylic and then to use a double-molding procedure to produce the poly(dimethylsiloxane) (PDMS) substrates used in our previous work (7, 10). 3D printing is also significantly easier and less expensive than creating substrates from etched silicon wafers as used by Sarles (15). The fabrication time is further saved by

designing the CAD file such that each mold can be used to produce a batch of substrates, with each substrate having a unique compartment geometry for defining the hydrogel shape (Figure 1b).

The design of the substrate used to house assemblies of lipid-encased hydrogels is based on a previous design presented during the introduction of the RAM (7) that features an upper reservoir and lower compartments for holding the aqueous volumes (Figure 1c). The upper reservoir is used to contain additional oil when used in an open fashion (without a cap) (7) but can also be left empty and plugged with a solid cap to produce fully encapsulated assemblies (10). Substrates used in this study are made from a flexible, transparent PU (Clear Flex 50, Smooth-On) to eliminate the problem of absorption of hydrocarbon solvents commonly encountered with PDMS (37). The tighter cross-linking of the PU rubber prevents absorption of the oil phase yet is still hydrophobic enough that the hydrogels do not readily wet the PU in the presence of oil. As with our previous work, mechanical flexibility of the substrate is an important parameter in the substrate design because the RAM uses an applied force on the substrate to modulate the dimensions of an aperture that separates the adjacent lower compartments. These controlled deformations are used to attach, separate, and reattach lipid-encased aqueous volumes for inducing and controlling interface bilayer formation.

Materials. A solution of lipid vesicles, consisting of 2 mg/mL diphytanoyl phosphocholine (DPhPC) phospholipid vesicles (purchased as lyophilized powder from Avanti Polar Lipids, Inc.) suspended in 500 mM KCl (Sigma) and a 10 mM 3-(N-morpholino)propanesulfonic acid (MOPS; Sigma), pH 7, buffer solution, is prepared and stored as described elsewhere (11). Hexadecane (99%, Sigma) is used without further purification as the oil in this study. Alamethicin channels (A.G. Scientific) from *Trichoderma viride* are stored in ethanol (Sigma) at 0.1% (w/v), and this stock solution is diluted further in the lipid vesicle solution to a final concentration of 50 ng/mL.

The poly(ethylene glycol) dimethacrylate polymer (PEG-DMA; MW = 1000 g/mol) purchased from PolySciences, Inc., is used as received as the hydrogel precursor. The free-radical photoinitiator used in this study, Irgacure 2959, was obtained as a gift from Ciba. Stock hydrogel solutions with concentrations of 20% (w/v), 80% (w/v), and 160% (w/v) PEG-DMA are prepared in a 500 mM KCl and 10 mM MOPS, pH 7, electrolyte solution and contain 0.5% (w/v) Irgacure 2959. Aqueous lipid—hydrogel mixtures consist of a 1:1 (v/v) mixture of a PEG-DMA stock solution and a lipid vesicle stock solution to final PEG concentrations of 10%, 40%, and 80% (w/v) PEG-DMA, respectively, 0.25% (w/v) photoinitiator, and 1 mg/mL DPhPC lipid vesicles in 500 mM KCl and 10 mM MOPS, pH 7. For tests requiring alamethicin, the final aqueous lipid—hydrogel—protein mixture contains 25 ng/mL alamethicin.

Gel Polymerization. Lipid—hydrogel mixtures are solidified through free-radical photopolymerization upon exposure to UV light using a hand-held UV spotlight (LED-100, Electro-Lite Corp.). Photopolymerization is prescribed for 3 min at an approximate distance of 2 mm from the 1 W, 365 nm source, which transforms the liquid volumes into water-swollen hydrogels.

Bilayer Formation and Recordings. Interface bilayers are formed in a PU substrate using the RAM (7). First, 40 μL of oil is pipetted into the open well of the PU substrate. Then, 600 nL of an aqueous lipid—hydrogel—protein solution is added to the droplet compartments such that the single aqueous volume spans both compartments and is pierced by both Ag/AgCl electrodes (125 μm diameter). The substrate is subsequently squeezed by hand either using a pair of stainless steel forceps or using a probe attached to a motorized micromanipulator (SM325, WPI, Inc.) in order to divide the aqueous volume into multiple volumes. The applied force is held for several seconds after separation in order to allow for monolayer formation at
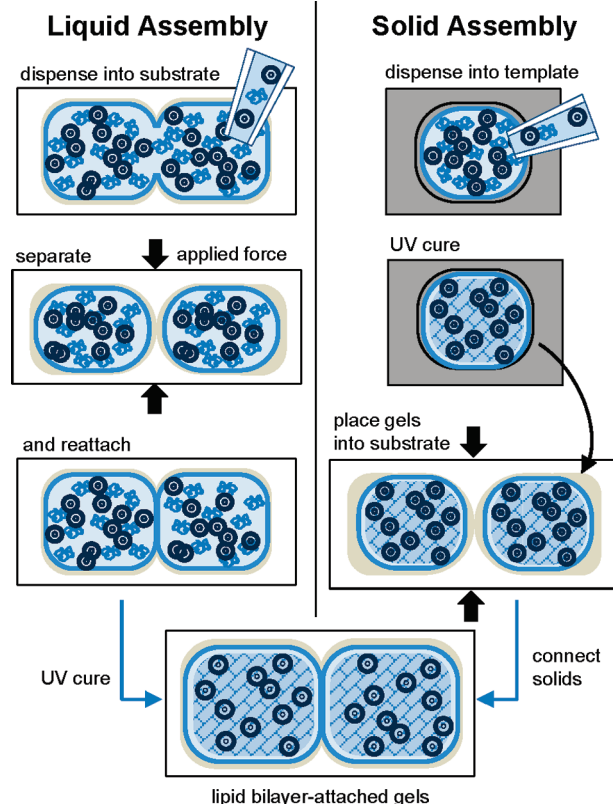
10% (w/v) PEG   40% (w/v) PEG

(a)   (b)

1mm

(c)

solid *VT* gels
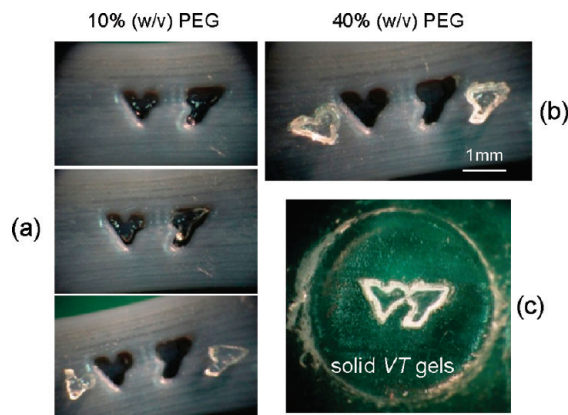
FIGURE 2. Photopolymerization of hydrogel precursors either pre-formed in the compartments designed into the printed template (a and b) or formed in situ in the PU substrate molded from the same template (c): (a) a gel concentration of 10% (w/v) PEG produces very soft, flexible gels in the shape of the compartment, (b and c) while a 40% (w/v) PEG concentration results in a more mechanically robust gel. Less shrinkage is seen in these samples. Some water evaporation occurs when gels are exposed to air during molding.

the oil/water interface of each volume. The separated volumes come into contact upon removal of the applied force, and interface bilayer formation occurs spontaneously within 1−2 min of initial contact. Bilayers formed to make single-channel measurements of alamethicin channels are consistently sized to have capacitances of approximately 100 pF (<150 μm equivalent diameter) by using the micromanipulator to control the attachment between the adjacent volumes.

Capacitance measurements of bilayer formation are obtained with the Ag/AgCl electrodes using an AxoPatch200B and a Digidata 1440A (Molecular Devices) to measure the square-wave current (sampled at 50 kHz and low-pass-filtered at 1 kHz) induced by an externally generated, 10 mV triangular voltage waveform at 100 Hz (the output of a Hewlett-Packard 3314A function generator). Single-channel current recordings for bilayers containing alamethicin are sampled at 250 kHz with low-pass filtering at 1 kHz. Bilayer rupture measurements are also performed using the AxoPatch by slowly increasing the applied holding potential until the membrane ruptures. A Canon Pow-erShot G6 digital camera connected to an AxioVert 40CFL inverted microscope is used to obtain digital images of the aqueous volumes in the PU substrates. All recordings are performed in a faraday cage for electrical shielding.

RESULTS AND DISCUSSION

Hydrogel Polymerization. The fabrication of hydro-gels swollen with a lipid vesicle solution is performed by the incorporation of PEG-DMA polymers and a photoinitiator into the DPhPC lipid vesicle solution. The photoinitiator absorbs energy from UV light, creating free radicals that initiate bulk polymerization, or cross-linking, of the water-soluble PEG polymers (24, 20). Per the type and amount of photoinitiator and PEG incorporated into the aqueous vol-umes in this work, gels are cured in this study with 3 min of direct (<5 mm separation) exposure to a 1 W LED UV light source. UV cross-linking produces solidified, water-swollen gels, where the mechanical and swelling properties of the gelled material are related to the cross-linking density (20, 21, 38). Hydrogels produced in this study are either solidified in a separate mold (Figure 2a,b) and then placed into the substrate compartment or directly polymerized in

Liquid Assembly

dispense into substrate

separate   applied force

and reattach

UV cure

Solid Assembly

dispense into template

UV cure

place gels into substrate

connect solids

lipid bilayer-attached gels

FIGURE 3. Bilayer formation between lipid-encased hydrogels oc-curring in two ways: through liquid assembly in which the bilayer is first formed between liquid mixtures of the hydrogel precursor and a lipid solution or after solidification between water-swollen gels. In both cases, the RAM is used to position and attach adjacent aqueous volumes.

the encapsulating PU substrate such as the *VT*-shaped gels shown in Figure 2c. Unlike liquid droplets used in construct-ing liquid assemblies such as DIBs, the solid nature of the polymerized gel structures allows for the volumes to take on nonspherical shapes. Solidified gels can also be manipu-lated in ways different from the liquid volumes and even removed entirely from the oil phase prior to bilayer forma-tion (Figures 2b and 3). In air, water-swollen hydrogels dehydrate within a few minutes. However, because these structures can be rehydrated with different types of aqueous solutions, hydrogel formation can occur as an independent step of forming material systems that use swollen hydrogels containing biomolecules and many types of hydrogels (in-cluding agarose, gelatin, etc.) can be used in addition to photocurable polymers such as PEG.

The cross-linking density of the hydrogel is adjusted by varying the molecular weight or loading percentage of the polymer in the solution. In this work, three different gel concentrations are studied for hydrogel polymerization: 10%, 40%, and 80% (w/v) PEG-DMA (MW = 1000) and 0.25% (w/v) photoinitiator suspended in an aqueous lipid vesicle stock solution. A mass percentage of 10% PEG-DMA is comparable to those used for the encapsulation of sus-pended lipid bilayers (30−32), while the two higher percent-ages chosen encompass and extend past the typical range for the construction of hydrogels used as tissure scaffolds (39) and biosensors (23, 28). A qualitative examination of

the gels shows that, at the lowest concentration of 10 % (w/v) PEG and 0.25 % (w/v) photoinitiator, the solidified gels remain highly compliant and are surrounded by a visible liquid sheath of an aqueous lipid solution. At the highest concentration [80 % (w/v) PEG and 0.25 % (w/v) photoinitiator], the cross-linked gel structure is more rigid and, with less water present, does not have a visible excess of liquid that surrounds the solid core.

Interface Bilayer Formation. The formation of interface bilayers between lipid-encased hydrogels can occur with the aqueous volumes either in the liquid phase or after the gels are solidified, as shown in Figure 3. In the first method, the aqueous mixture of phospholipids and a gel precursor is dispensed into oil contained in the substrate, where it is then separated and reattached using the RAM to induce bilayer formation. Then, through UV curing, the aqueous volumes on both sides of the membrane are solidified. This first approach is used primarily in this paper because it is desired to understand the effects of the gel phase on bilayer formation and protein function both before and after UV curing.

The second approach shown in Figure 3 is to first cure the hydrogel–lipid mixture using a template to shape the volume. The solid, water-swollen gels are then lifted out of the template and placed into adjacent compartments of the PU substrate, whereby via the RAM, the gels are gently brought into contact to initiate bilayer formation. Unlike the assembly of interface bilayers between liquid aqueous volumes, the latter approach enables the gels to be precured (with or without biomolecules present), dehydrated, and stored and then rehydrated prior to bilayer formation.

By connecting lipid-encased hydrogels contained in oil, an interface lipid bilayer forms spontaneously when excess oil is excreted from between the opposing lipid monolayers surrounding each gel (Figure 4a). This process produces liquid-supported membranes like DIBs (9) in which the bilayer is not directly assembled on a solid substrate such as those found in the formation of traditional planar bilayer lipid membranes (40–42). As a result, liquid-supported interface bilayers are known to last for days to weeks (9), whereas supported lipid bilayers may only last a few hours (43, 44).

Using the *liquid assembly* approach illustrated in Figure 3, a lipid bilayer is assembled in the PU substrate between two aqueous volumes that contain a mixture of lipid vesicles, PEG-DMA, and photoinitiator. The mixture is first injected into the oil-filled substrate, whereupon self-assembly leads to lipid monolayer formation at the oil/water interface around each aqueous volume. We observe that the addition of PEG-DMA and the photoinitiator to the aqueous lipid solution does make for a more viscous aqueous phase; however, the viscosity was not measured herein and across the concentration range tested, the increased viscosity does not inhibit or change the methods of bilayer formation. In its simplest operation, the RAM allows one to simply squeeze and release the substrate in order to form a bilayer, where the resulting interface dimensions are dictated by the un-
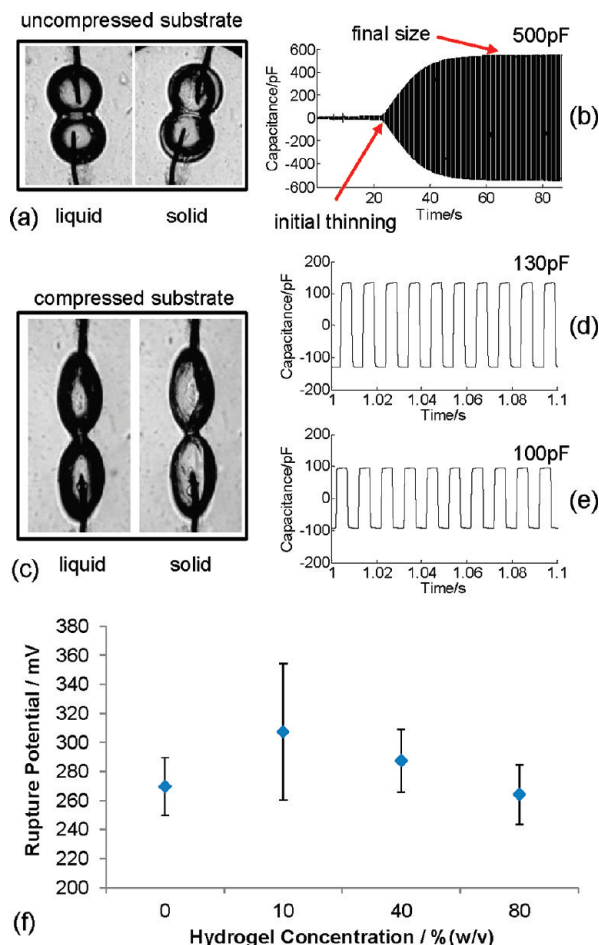
FIGURE 4. (a) Large interface formed between adjacent aqueous volumes in both the liquid (left) and solid (right) states when the substrate is not compressed after bilayer formation. (b) Real-time capacitance measurements used to monitor bilayer thinning and estimate the final size of the interface. (c) Compression of the substrate enabling formation of a much smaller interface bilayer, both before (left) and after (right) photopolymerization of the gel. (d and e) Square-wave capacitance measurements of this interface reveal that the area of the bilayer, which is directly related to capacitance, shrinks upon gel solidification. (f) Lipid bilayers formed between both liquid-phase lipid solutions (with no PEG) and lipid-encased gels exhibit rupture potentials between 260 and 300 mV.

compressed dimensions of the substrate (Figure 4b). However, a micromanipulator is used to control the aperture opening in tests where obtaining a single-channel protein measurement interface demands a smaller bilayer (<200 μm diameter) to reduce the capacitive noise from the membrane. Bilayer formation occurs spontaneously following the removal of excess oil from between the opposing monolayers as the volumes come into contact within the substrate (Figure 4c). The initial bilayer thinning, denoted by the sudden increase in the magnitude of the measured capacitance at ~22 s, and growth of the area of the interface are shown for a large bilayer. The capacitance measurements show that the bilayer size can be regulated from a maximum value of nearly 500 pF (~325 μm equivalent diameter) down to 100 pF (~145 μm), even for the same volumes of aqueous solution in the substrate compartments.

Lipid bilayers formed between aqueous lipid–hydrogel mixtures at all three PEG concentrations exhibit gigaohm

seals and last several hours while routinely enduring applied potentials greater than 150 mV without rupturing. We note that long-term testing of bilayers adjoining liquid-state aqueous volumes containing PEG-DMA is not performed because UV polymerization is prescribed to produce cured hydrogels.

An important finding of our work is that interface bilayers survive the UV polymerization step required to form cross-linked gels within the aqueous phases. This result reveals that the fluidity of the membrane (and of each lipid monolayer that encases the gels) is maintained throughout and even after the cross-linking process for all three PEG concentrations. While cured gels are not removed from the substrate to verify bulk solidification, we observe that, following UV exposure, the solidified aqueous phases do not conform to the substrate compartments like a liquid phase. Rather, as the substrate is compressed and relaxed, the volumes maintain a constant shape. Visual changes of the aqueous phases are also observed; the water-swollen hydrogels shown in Figure 4b,c appear slightly striated compared to their precured liquid state. Control tests performed with aqueous volumes that do not contain PEG-DMA polymer provide additional proof that the bilayer alone is not affected by the UV exposure and that no solidification is observed when the hydrogel precursor and photoinitiator are not present.

The rupture potentials of bilayers formed between connected hydrogel volumes are also measured in order to help understand the physical nature of the interface. Figure 4f shows that the rupture potentials of bilayers formed between aqueous volumes with and without PEG range from 260 to 320 mV, which are consistent with DIBs (45) and planar bilayers formed across the pores of a solid substrate (46). These results, along with observations of the cured aqueous volumes during testing, suggest that the gel structure does not directly interact with (or stabilize) the bilayer. Instead, a thin layer of water exists between the membrane and the PEG gel. The thickness of the water barrier is not measured in this study but could be controlled by tailoring of the maximum swelling ratio of a given hydrogel (20) and the amount of water incorporated into the initial hydrogel−lipid mixture. In this study, the fact that a thin layer of water is preserved between the bilayer and gel creates a favorable condition in which the membrane fluidity and macroscopic solidity of the material assembly can be controlled independently.

Gigaohm electrical resistances of bilayers formed between aqueous lipid−hydrogel mixtures enable measurement of single-channel protein currents (42, 46, 47). Alamethicin peptides, produced by the fungus *T. viride*, are added to the aqueous lipid−hydrogel mixtures (20 ng/mL final peptide concentration) used to form the bilayer. It is well established that application of a voltage across the bilayer drives adsorbed alamethicin peptides from the surface of the membrane through its thickness, where multiple peptides ($4 > n > 12$) can aggregate to form conductive channels (48−51). Figure 5 is a representative characterization of one such bilayer containing alamethicin and formed with a 40%

(w/v) PEG solution. The measured current traces indicate that while the first few conductance states of alamethicin are readily seen prior to polymerization (Figure 5a), channels consistently reach the third and fourth conductance states following solidification (Figure 5b). Additionally, photopolymerization increases the resistance, R, of the bilayer by more than a factor of 2 from 6.5 GΩ in the liquid state to approximately 17 GΩ after polymerization. Phrased differently, solidification of the gel reduces the amount of current that passes through the bilayer when no channels are gating, called the closed-state current, i_c. Average measured channel conductances for alamethicin after photopolymerization are 0.12, 0.48, 0.92, 1.5, and 2.3 nS, respectively, for the first five conductance states (O_{1-5}). Agreement in the measured conductances with those measured by Sansom (52) in a 0.5 M KCl electrolyte provides convincing evidence that the measured current is, in fact, alamethicin gating and not an effect of the hydrogel.

Just as liquid phases can be separated and reattached using the RAM (7), solidified gels can also be separated and reconnected to form a new bilayer interface. The real-time capacitance measurement shown in Figure 5c shows that, by compression of the substrate to reclose the aperture, the bilayer is completely unzipped, whereby the capacitance drops to near zero. After a few seconds of separation, the aperture is reopened to form a new bilayer interface, marked by the subsequent rise and plateau of the capacitance. The magnitude of the capacitance before separation and after re-formation indicates that the bilayer formed between these gels has approximately the same size.

The complete separation and reattachment of solidified gels also points toward the existence of a thin layer of water between the cross-linked gel and the interface bilayer. The impact of this result is that presolidified hydrogels can be formed in situ (as shown here) or solidified separately and placed into the substrate to form an interface bilayer. In this manner, gels can be shaped and stored for later use in the building of specific assemblies. The data presented here also show that connecting water-swollen solids rather than liquids still produces a high-quality, durable lipid bilayer. Current recordings immediately after connecting solidified gels to form a fresh interface bilayer, and those taken 2 days later on the same bilayer, show that membrane resistance remains greater than 10 GΩ, which allows for distinct changes in the channel conductance to be measured (Figure 5d,e). Finally, in a separate control experiment for the same PEG concentration, current recordings show that without alamethicin no gating behavior is observed (Figure 5f,g). These measurements confirm that the presence of the PEG does not contribute to the measured electrical response of the bilayer either before or after solidification.

The addition of polymeric hydrogels into the aqueous volumes also produces mechanically robust membranes. The current traces shown in Figure 5h,i demonstrate that a bilayer formed between two 40% (w/v) hydrogels and contained within the PU substrate is maintained even as the substrate is dropped from a height of 5.1 cm. The spikes in
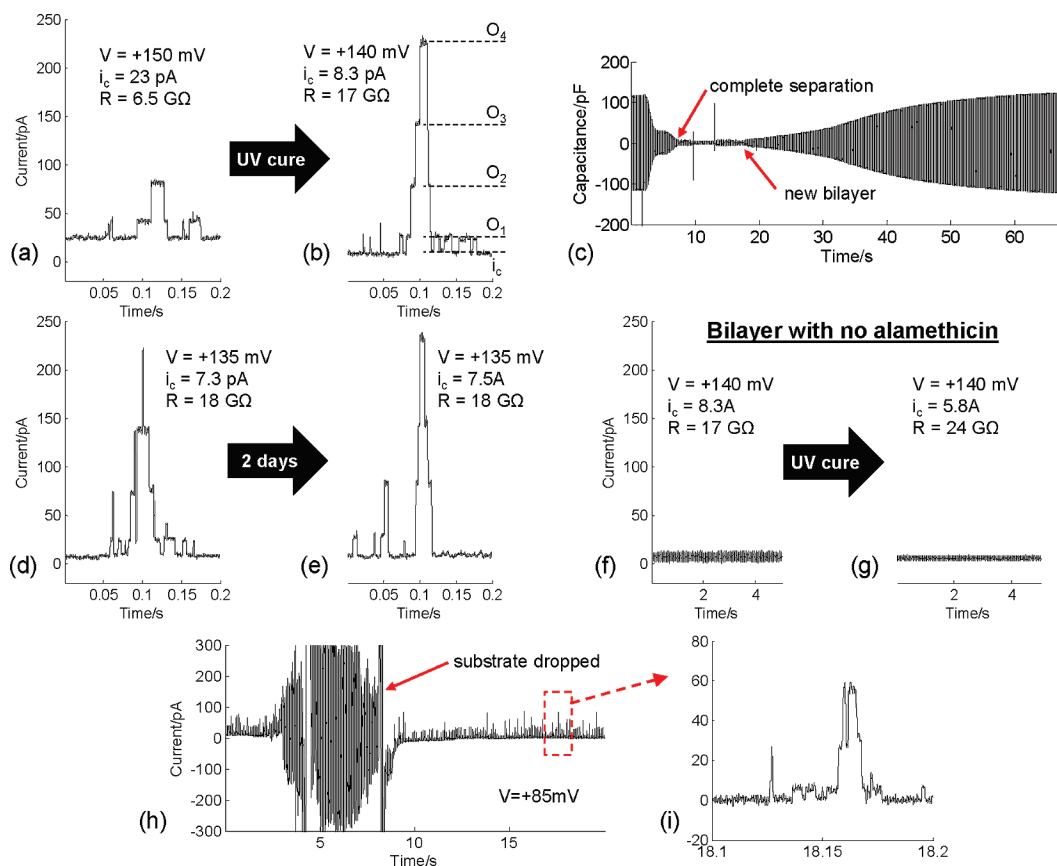
FIGURE 5. Successive single-channel recordings of alamethicin channels in an interface bilayer formed from an aqueous lipid−hydrogel−protein mixture containing 40% PEG-DMA shown for the presolidified liquid state (a) and in the solid state after UV irradiation (b). (c) Real-time capacitance measurement demonstrating that solidified biomolecular assemblies can be fully detached and then later reconnected to form fresh interface bilayers using the RAM. Alamethicin gating is seen in the single-channel recordings after formation of a new interface between solidified gels (d) and again 2 days later (e). Current recordings before (f) and after (g) UV curing are shown for a bilayer formed using a 40% (w/v) PEG−lipid solution that does not contain alamethicin channels. (h) Continuous current recordings of alamethicin channels gating in a lipid bilayer formed between hydrogels held in the PU substrate show that the bilayer survives having the PU substrate picked up and then dropped from a height of 5 cm at the 8-s mark. The noisy current measured from 3 to 8 s is caused when the substrate is handled. (i) Single-channel alamethicin transitions measured after impact confirm that the bilayer survives the drop.

the current shown before and after the substrate is manually picked up and dropped correspond to alamethicin gating (250 ng/mL final concentration) at an applied voltage of 85 mV. Membranes tested in this fashion typically survive repeated (>4) drops from heights ranging from 4 to 8 cm, where impact velocities of the substrate dropped from 5 cm approach 1 m/s. Because we believe that a thin layer of water exists between the membrane and the cross-linked gel structure, we attribute the observed durability to both the use of an encapsulating substrate designed to confine the contents (10) and the hydrophilic nature of the gel. Both act to minimize gross movements of the water on both sides of the bilayer. It should be noted that pure liquid-phase aqueous volumes supported in the substrate also survive similar drops; however, the result with connected gels further supports that the aqueous phase can be solidified without reducing the performance of the bilayer.

Effects of Solidification. The measurements of protein insertion and membrane rupture and observations of reconfigurability and durability discussed above suggest that the gel produces few if any changes in the structure or stabilization of the bilayer. This is a desired effect because a goal in this study is to demonstrate that the aqueous phases

can be modified via hydrogels without detriment to the interface. However, the data do reflect that bulk solidification of the gel on both sides of the interface can affect transport through proteins that reside in the bilayer that adjoins these water-swollen solids. These changes are readily observed as a result of the formation of the bilayer prior to photopolymerization, and they illustrate the advantages of membrane formation after hydrogel solidification.

Electrical measurements of the bilayer reveal that the liquid-to-solid transformation of the aqueous phases on both sides of the membrane can affect both the size and quality of the interface. Postcure capacitance measurements (Figure 4e,f) show that an interface bilayer shrinks slightly during the solidification process. Additional capacitance measurements (not shown) during UV exposure confirm that the area of the interface decreases during solidification. We attribute this reduction in the interfacial size (typically 5−20%) to gel shrinkage (53) and reorientation of the aqueous solid within the substrate compartments during polymerization that acts to pull away at the bilayer interface, unzipping it slightly.

Prior to gel formation, the closed-state current measurements indicate that the presence of dispersed PEG-DMA molecules results in lower bilayer resistances, or "leakage".
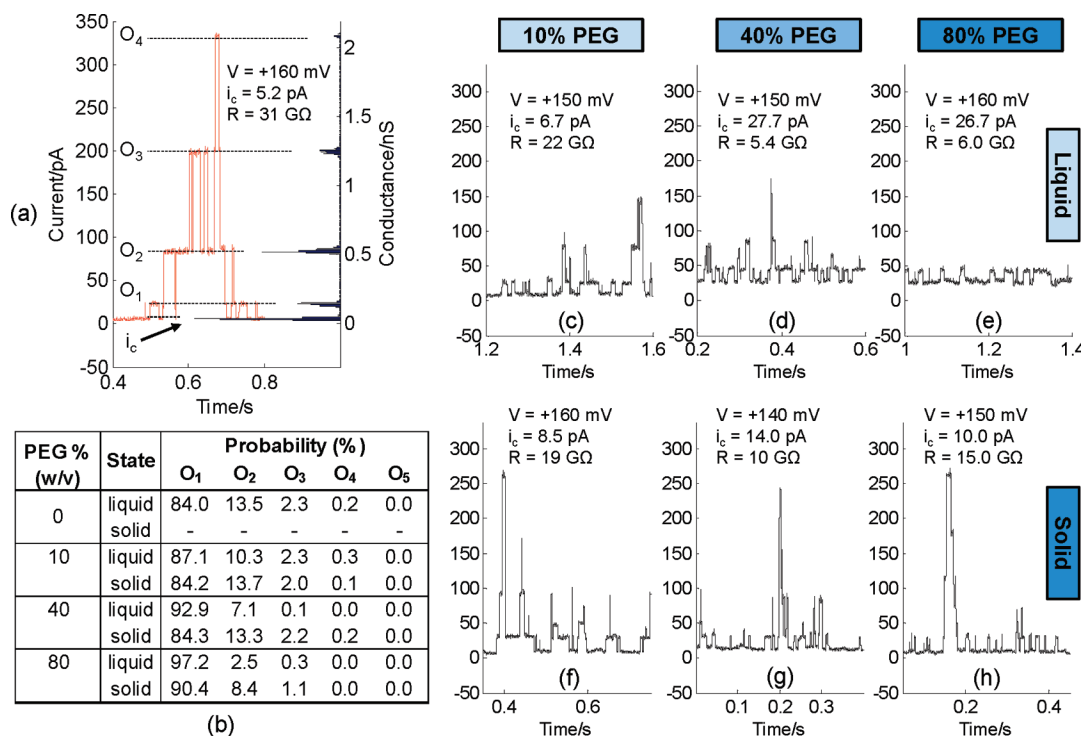
FIGURE 6. Single-channel recordings of alamethicin channels illustrating the effects of the PEG concentration (organized by columns) on the gating behavior of the channels. The top row of current traces (a and c–e) represents measurements taken with the aqueous volumes in the liquid state, while the bottom row represents subsequent recordings for the same respective membranes after 3 min of UV exposure (f–h). Population analysis of alamethicin gating over long time frames (>60 s) is provided for the four concentrations of PEG before and after UV curing (b). The applied voltage, closed-state current, and approximate membrane resistance are provided for each trace. Note: all axes share equal tick mark spacing.

This effect, which is more pronounced at 40% and 80% gel loading, is attributed to the amphiphilic structure of the short-chained PEG-DMA monomers, which may inhibit lipid monolayer formation and packing either directly by being present at or near the oil/water interface or indirectly by slowing phospholipid absorption to the interface (54). However, photopolymerization of the gel helps to restore a better electrical seal between adjacent gels even at high gel concentrations. Figures 5a,b and 6c,d,f,g show that, for both 40% and 80% PEG loading, the resistance of the membrane increases (and the closed-state current, i_c, decreases) as a result of UV irradiation. This change in the bilayer resistance is attributed to the reduced competition that freely dispersed PEG-DMA polymers may have on monolayer formation and through expulsion of excess vesicle solution from within the cross-linked gel upon network formation. The physical formation of the gel structure effectively distributes lipid vesicles closer to the surrounding oil/water interface, which, in turn, results in better monolayer packing and higher bilayer resistance. Conveniently, the results show that concentrations as high as 80% (w/v) PEG, far beyond levels typically used to produce gels of reasonable mechanical strength (25, 28, 39), still produce bilayers with gigaohm seals both prior to and following photopolymerization.

The second effect that gel solidification has on the system is in reducing the interactions between dispersed polymers in the solution and the lipid membrane. In this study, we use single-channel measurements of alamethicin channels incorporated into the interface bilayers to confirm the bilayer

structure and understand the effects of both the hydrogel precursor present prior to photopolymerization and the gelled network following UV exposure. The traces shown in Figure 6 compare representative current recordings for a PEG-free interface bilayer in the liquid state and for three bilayers formed with aqueous mixtures of PEG and lipids both prior to (c–e) and following (f–h) UV exposure.

The representative current traces shown in Figure 6 qualitatively show that alamethicin peptides insert into bilayers formed in the close vicinity of the gel, where the higher conductance states are more readily achieved at low PEG concentrations in the liquid state and prior to solidification for aqueous phases containing more than 10% (w/v) PEG. Quantitatively, the effect of the gel on the gating activity of alamethicin can be divided into two separate categories: osmotic pressure-induced changes in the channel gating behavior and conductivity changes caused by the formation of a cross-linked hydrogel.

We note that while the following discussion builds on previous works that studied the effect of unfunctionalized PEG dispersed in the aqueous phase on the alamethicin channel gating, these works did not produce cross-linked gels on either side of the membrane. Our study follows the behavior of voltage-gated alamethicin channels through solidification in order to understand what effects the cross-linked gel has on the transport properties of biomolecules within the bilayer.

Analysis of single-channel alamethicin recordings presented in Figure 6b shows that higher PEG-DMA concentra-

tions in the liquid state result in a reduced number conductance states for alamethicin. Prior to solidification, our findings are consistent with what Vodyanoy et al. saw while using dispersed PEG polymers to probe the conductance states of alamethicin (55). The conclusions of their studies stated that the exclusion of large hydrophilic PEG polymers from alamethicin channels results in an altered solution conductivity and an increased osmotic pressure on the channel, which suppresses its tendency to reach higher order conductance levels. Because osmotic stress on a channel is a function of the channel volume, higher-order states are more affected than lower-order states by the exclusion of PEG. The control case with 0 % PEG, shown in Figure 6a, verifies that, in the absence of PEG, higher-order states can be achieved. In comparison, our data also suggest that similar behavior is occurring in that first and second conductance states are still readily observed 10 % and 40 % PEG concentrations in the liquid phase (Figure 6c,d), while only the first conductance state appears for 80 % (w/v) PEG (Figure 6e). Vodyanoy et al. showed that these effects are related to the size of the PEG polymers (55). Smaller chains (MW < 1000 g/mol) are not excluded as easily from the channel volume and therefore have less of an effect on gating as larger nonpenetrating molecules.

These effects are less prevalent after gel formation, where ion channels readily reach the third and fourth conductance states (Figure 6f—h) regardless of the gel concentration. Analysis of the population of each conductance level provided in Figure 6b quantitatively shows that solidification of the gels increases the probability that channels reach the higher-order states when they open. Specifically, the data show that, for 10 % and 40 % PEG, the population states after curing closely resemble the weighting of the conductance states measured for liquid aqueous volumes with 0 % PEG. Osmotic stress induced on the channels by the gel after polymerization may still provide some measure of channel suppression; note the reduced burst duration during the open states for 40 % and 80 % PEG concentrations compared to 0 % PEG. However, this effect is lessened by the fact that, through polymerization, the bilayer (and alamethicin channels contained within) has less interaction with PEG polymers. Again, the data suggest that a thin layer of excess water that sheaths the water-swollen gel allows the channels to gate more freely.

The second category of gel effects on the bilayer is that of altered electrolyte conductivity both inside and outside of the channel. Bezrukov et al. showed that neutral PEG polymers dispersed in the aqueous phase affect the conductivity both within the alamethicin channel and in the bulk solution (56) depending on the size of the PEG polymers. Short-chained PEG (MW < 2000) penetrate the channel interior, resulting in a reduced electrolyte conductivity (and conductance) within the channel. Larger PEG molecules (MW > 2000), which are unable to occupy the channel interior, have the opposite effect; the bulk electrolyte conductivity is reduced, and the conductance of the channel increases. These effects are also concentration-dependent, with changes

Table 1. Average Measured Conductance States for Alamethicin Channels in the Presence of a Cured PEG Hydrogel Swollen with 0.5 M KCl

PEG % (w/v)	nominal values (nS)					normalized values (per O1)				
	O_1	O_2	O_3	O_4	O_5	O_1	O_2	O_3	O_4	O_5
0	0.12	0.58	1.32	2.14	3.01	1	4.7	10.7	17.3	24.4
10	0.13	0.51	1.03	1.65	2.32	1	4.0	8.1	13.0	18.3
40	0.12	0.48	0.92	1.52	2.28	1	3.9	7.6	12.5	18.7
80	0.12	0.42	0.72	1.17	1.56	1	3.4	5.9	9.5	12.7
0	0.09^a	2.0^a	2.7^a	0.55^a	1.2^a	1	6.1	13.3	22.2	30.0

^{a} Conductance values compiled from: Sansom, M. S. *Prog. Biophys. Mol. Biol.* **1991**, *55*, 139−235.

in the solution conductivity occurring for higher PEG loading. In addition to ionic interactions with an electrolyte solution that may alter the solution conductivity, the gel network creates a more tortuous pathway for ion movement within the gel.

The data presented in Table 1 summarize the measured nominal and normalized conductance levels of alamethicin channels for varying amounts of polymerized hydrogel. These values compare well to the first five conductance states of alamethicin in 500 mM KCl measured by Sansom (52). The results show that while the first channel conductance is not greatly affected by the polymer gel, the higher-order conductance levels ($n > 1$) demonstrate a decreased conductance for increasing amounts of cross-linked PEG. The ratio of the conductance levels, however, remains nearly constant for all PEG loadings, providing additional confirmation that alamethicin is still gating despite shorter bursts and reduced conductivity. Conductance levels of alamethicin channels for liquid-phase aqueous volumes are not shown because the reduced gating activity prevented adequate analysis of the higher-order conductance states for PEG concentrations greater than 10 %. After polymerization, however, recordings show that even the sixth and seventh conductance states of the channels are visible (though not shown in Table 1).

CONCLUSIONS

The results of this study allow us to conclude that lipid bilayers can be formed using the RAM between water-swollen hydrogels both in the precured liquid (dispersed) state and following solidification as a cross-linked polymer network. The results of the experiments on aqueous volumes consisting of 10 %, 40 %, and 80 % (w/v) PEG-DMA also validate that a wide range of gel concentrations can be used. These data points further allow us to conclude that both the chemical composition and the mechanical properties of solidified biomolecular assemblies can be tailored using hydrogels without disrupting the bilayer formation or durability. Observations of lipid-encased hydrogel volumes solidified after the initial bilayer formation suggest that the hydrogel−lipid mixture used in this study contains more water than the gels can uptake, leaving additional water to coat the cured gel structures. Bilayer rupture measurements with and without PEG and drop tests of solidified gel volumes

indicate that this thin layer of water surrounding the swollen gel and adjacent to the membrane serves to preserve the fluidity and durability of the interface. The measured conductance states of alamethicin channels also demonstrate that proteins incorporated into the hydrogel—lipid mixture can insert into bilayers sandwiched between cured gels. The presence of dispersed hydrogel precursors prior to UV curing does affect the system, where dissolved PEG-DMA in the aqueous volumes was found to affect the conductivity, viscosity, and osmotic pressure of these aqueous phases. Specifically, single-channel recordings of alamethicin peptide pores reveal that an increased osmotic pressure suppresses the ability for the channels to form and maintain higher-order conductance states. Gel solidification through UV curing reduces these effects on ion transport through the pores, where population analysis of alamethicin gating shows that channels behave more like those contained in bilayers with no PEG present in the aqueous volumes. Finally, the fact that lipid-encased hydrogels can be attached, separated, and reattached to form new interface bilayers demonstrates that solidified biomolecular assemblies retain the configurability demonstrated initially with DIBs.

REFERENCES AND NOTES

(1) Bayley, H.; Cremer, P. S. *Nature* **2001**, *413*, 226–230.

(2) Guan, X.; Gu, L.-Q.; Cheley, S.; Braha, O.; Bayley, H. *ChemBioChem* **2005**, *6*, 1875–1881.

(3) Ervin, E. N.; White, R. J.; White, H. S. *Anal. Chem.* **2009**, *81*, 533–537.

(4) Astier, Y.; Braha, O.; Bayley, H. *J. Am. Chem. Soc.* **2006**, *128*, 1705–1710.

(5) Srisa-Art, M.; deMello, A. J.; Edel, J. B. *Chem. Commun.* **2009**, 6548–6550.

(6) Gu, L.-Q.; Shim, J. W. *Analyst* **2010**, *135*, 441–451.

(7) Sarles, S. A.; Leo, D. J. *Anal. Chem.* **2010**, *82*, 959–966.

(8) Funakoshi, K.; Suzuki, H.; Takeuchi, S. *Anal. Chem.* **2006**, *78*, 8169–8174.

(9) Holden, M. A.; Needham, D.; Bayley, H. *J. Am. Chem. Soc.* **2007**, *129*, 8650–8655.

(10) Sarles, S. A.; Leo, D. J. *Lab Chip* **2010**, *10*, 710–717.

(11) Hwang, W. L.; Chen, M.; Cronin, B.; Holden, M. A.; Bayley, H. *J. Am. Chem. Soc.* **2008**, *130*, 5878–5879.

(12) Bayley, H.; Cronin, B.; Heron, A.; Holden, M. A.; Hwang, W. L.; Syeda, R.; Thompson, J.; Wallace, M. *Mol. BioSyst.* **2008**, *4*, 1191–1208.

(13) Syeda, R.; Holden, M. A.; Hwang, W. L.; Bayley, H. *J. Am. Chem. Soc.* **2008**, *130*, 15543–15548.

(14) Maglia, G.; Heron, A. J.; Hwang, W. L.; Holden, M. A.; Mikhailova, E.; Li, Q.; Cheley, S.; Bayley, H. *Nat. Nanotechnol.* **2009**, *4*, 437–440.

(15) Sarles, S. A. Physical Encapsulation of Interface Bilayers. Dissertation, Virginia Polytechnic Institute and State University, Blacksburg, VA, 2010.

(16) van der Zwan, E.; Schroën, K.; van Dijke, K.; Boom, R. *Colloids Surf., A* **2006**, *277*, 223–229.

(17) Lorenz, R. M.; Edgar, J. S.; Jeffries, G. D. M.; Chiu, D. T. *Anal. Chem.* **2006**, *78*, 6433–6439.

(18) Teh, S.-Y.; Lin, R.; Hung, L.-H.; Lee, A. P. *Lab Chip* **2008**, *8*, 198–220.

(19) Schaerli, Y.; Hollfelder, F. *Mol. BioSyst.* **2009**, *5*, 1392–1404.

(20) Peppas, N. A.; Keys, K. B.; Torres-Lugo, M.; Lowman, A. M. *J. Controlled Release* **1999**, *62*, 81–87.

(21) Lin-Gibson, S.; Jones, R. L.; Washburn, N. R.; Horkay, F. *Macromolecules* **2005**, *38*, 2897–2902.

(22) Liu, L.; Li, P.; Asher, S. A. *Nature* **1999**, *397*, 141–144.

(23) Lewis, C. L.; Choi, C.-H.; Lin, Y.; Lee, C.-S.; Yi, H. *Anal. Chem.* **2010**, *82*, 5851–5858.

(24) Nguyen, K. T.; West, J. L. *Biomaterials* **2002**, *23*, 4307–4314.

(25) Pfister, P. M.; Wendlandt, M.; Neuenschwander, P.; Suter, U. W. *Biomaterials* **2007**, *28*, 567–575.

(26) Kim, S. W.; Bae, Y. H.; Okano, T. *Pharm. Res.* **1992**, *9*, 283–290.

(27) Qiu, Y.; Park, K. *Adv. Drug Delivery Rev.* **2001**, *53*, 321–339.

(28) Meiring, J. E.; Schmid, M. J.; Grayson, S. M.; Rathsack, B. M.; Johnson, D. M.; Kirby, R.; Kannappan, R.; Manthiram, K.; Hsia, B.; Hogan, Z. L.; Ellington, A. D.; Pishko, M. V.; Willson, C. G. *Chem. Mater.* **2004**, *16*, 5574–5580.

(29) Peppas, N.; Hilt, J.; Khademhosseini, A.; Langer, R. *Adv. Mater.* **2006**, *18*, 1345–1360.

(30) Jeon, T.-J.; Malmstadt, N.; Schmidt, J. J. *J. Am. Chem. Soc.* **2006**, *128*, 42–43.

(31) Jeon, T.-J.; Malmstadt, N.; Schmidt, J. *Mechanical studies of hydrogel encapsulated membranes*; Materials Research Society: Warrendale, PA, 2006.

(32) Kang, X.-f.; Cheley, S.; Rice-Ficht, A. C.; Bayley, H. *J. Am. Chem. Soc.* **2007**, *129*, 4701–4705.

(33) Ide, T.; Kobayashi, T.; Hirano, M. *Anal. Chem.* **2008**, *80*, 7792–7795.

(34) Thompson, J. R.; Heron, A. J.; Santoso, Y.; Wallace, M. I. *Nano Lett.* **2007**, *7*, 3875–3878.

(35) Heron, A. J.; Thompson, J. R.; Mason, A. E.; Wallace, M. I. *J. Am. Chem. Soc.* **2007**, *129*, 16042–16047.

(36) Heron, A. J.; Thompson, J. R.; Cronin, B.; Bayley, H.; Wallace, M. I. *J. Am. Chem. Soc.* **2009**, *131*, 1652–1653.

(37) Lee, J. N.; Park, C.; Whitesides, G. M. *Anal. Chem.* **2003**, *75*, 6544–6554.

(38) Lin-Gibson, S.; Bencherif, S.; Cooper, J. A.; Wetzel, S. J.; Antonucci, J. M.; Vogel, B. M.; Horkay, F.; Washburn, N. R. *Biomacromolecules* **2004**, *5*, 1280–1287.

(39) Arcaute, K.; Ochoa, L.; Medina, F.; Elkins, C.; Mann, B.; Wicker, R. *Three-dimensional PEG hydrogel construct fabrication using stereolithography*; Materials Research Society: Warrendale, PA, 2005.

(40) Montal, M.; Mueller, P. *Proc. Natl. Acad. Sci. U.S.A.* **1972**, *69*, 3561–3566.

(41) White, S. H. *Biophys. J.* **1978**, *23*, 337–347.

(42) Romer, W.; Steinem, C. *Biophys. J.* **2004**, *86*, 955–965.

(43) Han, X.; Studer, A.; Sehr, H.; Geissbühler, I.; Di Berardino, M.; Winkler, F.; Tiefenauer, L. *Adv. Mater.* **2007**, *19*, 4466–4470.

(44) Reimhult, E.; Kumar, K. *Trends Biotechnol.* **2008**, *26*, 82–89.

(45) Sarles, S. A.; Bavarsad, P. G.; Leo, D. J. *Incorporation and characterization of biological molecules in droplet-interface bilayer networks for novel active systems*; SPIE Publications: Bellingham WA, 2009.

(46) Kresak, S.; Hianik, T.; Naumann, R. L. C. *Soft Matter* **2009**, *5*, 4021–4032.

(47) Wong, D.; Jeon, T.-J.; Schmidt, J. *Nanotechnology* **2006**, *17*, 3710.

(48) Vodyanoy, I.; Hall, J. E.; Vodyanoy, V. *Biophys. J.* **1988**, *53*, 649–658.

(49) Andrew Woolley, G.; Wallace, B. *J. Membr. Biol.* **1992**, *129*, 109–136.

(50) He, K.; Ludtke, S. J.; Heller, W. T.; Huang, H. W. *Biophys. J.* **1996**, *71*, 2669–2679.

(51) Bechinger, B. *J. Membr. Biol.* **1997**, *156*, 197–211.

(52) Sansom, M. S. *Prog. Biophys. Mol. Biol.* **1991**, *55*, 139–235.

(53) Hino, T.; Endo, T. *Macromolecules* **2003**, *36*, 5902–5904.

(54) Gehrhardt, H.; Mutter, M. *Polym. Bull.* **1987**, *18*, 487–493.

(55) Vodyanoy, I.; Bezrukov, S. M.; Parsegian, V. A. *Biophys. J.* **1993**, *65*, 2097–2105.

(56) Bezrukov, S. M.; Vodyanoy, I. *Biophys. J.* **1993**, *64*, 16–25.

AM100826S